BRICS TRANSPORT
VOL. 2 ISSUE 1 2023
TRANSPORT INFRASTRUCTURE
ИНФРАСТРУКТУРА ТРАНСПОРТА

Original article
UDC 625.033.34
doi: 10.46684/2023.1.4

Modulus of elasticity of non-ballasted track

Ksenia I. Ivanova[1]✉, Alexey F. Kolos[2], Xintong Wang[3]
[1, 2, 3] Emperor Alexander I St. Petersburg State Transport University (PGUPS); St. Petersburg, Russian Federation
[1] kivanova@pgups.ruv✉
[2] kolos2004@inbox.ru
[3] wangxintong@mail.ru

ABSTRACT The main stiffness properties that determine the stresses in the track structure components under loads from a moving train are the modulus of elasticity of the rail slab and the slab-track/rail correlation stiffness coefficient. These parameters have been investigated for a ballasted track and are well established today, in contrast to those of a non-ballasted track. This study aims at determining the stiffness characteristics of a non-ballasted track, comparing them with those of a ballasted track, and assessing their effect on the stress-strain state (SSS) of the elements of a non-ballasted track structure. Field experiments to measure the stresses in the track structure elements were carried out using strain-gauge methods. As a result of the experiments, the modulus of elasticity and the correlation stiffness coefficient of the rail slab and the rail were determined for the RHEDA2000 slab track system. The results obtained prove it possible to apply a rail-as-beam-on-elastic-foundation theory and to use well-established calculation methods for designing a non-ballasted track structure suitable for different operational conditions.

KEYWORDS: non-ballasted (ballastless) track; modulus of elasticity of rail slab; rail slab/rail correlation stiffness coefficient; RHEDA 2000 non-ballasted track design; model of beam on a continuous elastic foundation; strain-gauge method

For citation: Ivanova K.I., Kolos A.F., Wang X. Modulus of elasticity of non-ballasted track. *BRICS transport*. 2022;2(1):4. https://doi.org/10.46684/2023.1.4.

Научная статья

Упругие характеристики подрельсового основания безбалластного железнодорожного пути

К.И. Иванова[1]✉, А.Ф. Колос[2], С. Ван[3]
[1, 2, 3] Петербургский государственный университет путей сообщения Императора Александра I (ПГУПС); г. Санкт-Петербург, Россия
[1] kolos2004@inbox.ru✉
[2] kivanova@pgups.ru
[3] wangxintong@mail.ru

АННОТАЦИЯ Основными упругими характеристиками, определяющими значения напряжений в элементах конструкции верхнего строения пути под нагрузкой от движущегося поезда, являются модуль упругости подрельсового основания и коэффициент соотносительной жесткости подрельсового основания и рельса. Значения этих параметров для пути с ездой на балласте сегодня исследованы и хорошо известны, в отличие от безбалластного пути. Цель исследования — натурное определение упругих характеристик безбалластного железнодорожного пути, их сравнение с аналогичными характеристиками для пути на балласте и оценка воздействия данных характеристик на напряженно-деформированное состояние элементов верхнего строения безбалластного пути. Натурные испытания по измерению напряжений в элементах верхнего строения пути осуществлялись с помощью тензометрических методов. В результате экспериментов установлены значения модуля упругости подрельсового основания и коэффициента соотносительной жесткости подрельсового основания и рельса для безбалластной конструкции RHEDA2000. Полученные результаты дают возможность рассматривать рельс как балку, лежащую на сплошном упругом основании, применительно к безбалластному пути и использовать известные методы расчета для проектирования железнодорожного пути с устройством безбалластной конструкции в зависимости от условий эксплуатации.

КЛЮЧЕВЫЕ СЛОВА: безбалластный путь; модуль упругости подрельсового основания; коэффициент соотносительной жесткости подрельсового основания и рельса; конструкция безбалластного пути RHEDA 2000; модель балки, лежащей на сплошном упругом основании; тензометрический метод

Для цитирования: *Иванова К.И., Колос А.Ф., Ван С.* Упругие характеристики подрельсового основания безбалластного железнодорожного пути // Транспорт БРИКС. 2023. Т. 2. Вып. 1. Ст. 4. https://doi.org/10.46684/2023.1.4.

INTRODUCTION

At present, the railway transport in the Russian Federation has been developing due to the continuous expansion of the fast and high-speed railway networks and an increase in railway carrying capacity together with the growing volume of freight and passenger traffic. On sections with speeds above 160 km/h (on fast and high-speed sections), there is a worldwide practice of switching to slab track systems as the most low-maintenance and long-lasting (up to 50–60 years) structures [1]. Non-ballasted track systems require significant capital investment but they have a number of advantages over ballasted track structures. These advantages lie in the reduction of maintenance costs, improved train ride quality and passenger ride comfort as well as reduced fuel and energy consumption required for train traction and others [2].

World practices in the operation of non-ballasted track systems have shown their cost effectiveness under certain operational conditions [3]. There are more than 30 types of non-ballasted track systems in the world today, but choosing a certain system for specific operational conditions remains a complicated task [4]. One of the reasons is a lack of easy methods for calculating the stress-strain state (SSS) of a ballastless track, which would take into account the specifics of the designed structure, engineering and geological conditions of construction, operational conditions in the future, etc. The calculation methods known today are labour-intensive and require a considerable amount of input data. In addition, their application will be challenging for ordinary engineering personnel in design organisations due to their mathematical complexity. When comparing rail performance in ballasted and non-ballasted track structures, the rail can be modelled as a beam resting on a continuous elastic foundation [5]. Due to this method, it is possible to carry out the assessment of the track structure SSS using well-established theories and calculation methods.

The evaluation of the track elements SSS for a conventional ballasted track is carried out in accordance with the track stiffness calculation methods based on the above-stated assumption that a rail is a beam on an elastic foundation [6]. In accordance with these methods, the Schwedler-Zhuravsky theorem for the curved rail axis is applied

$$EI\frac{d^2y}{dx^2} = M \quad \text{или} \quad -EI\frac{d^4y}{dx^4} = \frac{d^2M}{dx^2} = q, \qquad (1)$$

where E is the modulus of elasticity of rail steel; I is the inertia moment of the rail cross-section in relation to its central horizontal axis passing through the centre of gravity of a section; y is the rail transverse elasticity under load; M is the bending moment; q is the rail slab performance.

In equation (1), a linear dependence between the rail transverse elasticity and the rail slab performance is defined and is expressed by the modulus of elasticity of the rail slab U

$$q = -U \cdot y. \qquad (2)$$

Integration of equation (1) with dependence (2) makes it possible to determine the rail transverse elasticity, the bending moment value and the rail pressure on the sleeper (formulae (3)) [7].

$$y = \frac{Pk}{2U}e^{-kx}(\cos kx + \sin kx),$$

$$M = \frac{P}{4k}e^{-kx}(\cos kx - \sin kx), \qquad (3)$$

$$Q = Uyl = \frac{Pkl}{2}e^{-kx}(\cos kx + \sin kx),$$

where l is the distance between sleeper axes; k is the correlation stiffness coefficient of the rail slab and the rail determined by the relation

$$k = \sqrt[4]{\frac{U}{4EI}}. \qquad (4)$$

According to formula (3), the bending moment is proportional to the ordinates of the influence line μ_kx that are defined by the relation (formula (5)). Graphically, μ_kx function is shown in *Fig. 1*. Fig. 1 also shows the position of the dynamic vertical forces acting from the rolling stock wheels on the rails.

$$\mu_{kx} = e^{-kx}(\cos kx - \sin kx). \qquad (5)$$

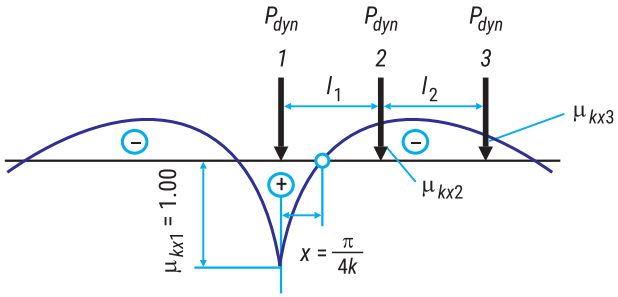

Fig. 1. Diagram showing the bending moment of a rail modelled as beam on a continuous elastic foundation

Fig. 1 shows that the bending moment line crosses the horizontal axis at points that have equal ordinates: $x = \pi/4k$, then, $x = 5\pi/4k$, etc. Thus, knowing the distances x it is possible to find experimentally the correlation stiffness coefficient of the rail slab and rail k, and further, using formula (4) and expressing U through k, to find the modulus of elasticity of the rail slab.

$$U = 4 \cdot E \cdot I \cdot k^4. \quad (6)$$

U and k are design characteristics of a railway track and have been well researched for a ballasted track structure [8]. The mean U-value for a ballasted track with reinforced concrete sleepers varies between 50–120 MPa; and for a track with timber sleepers, it is 20–30 MPa. The change in the values depends on the elastic properties of the rail pads, the sleeper layout, the elastic properties of the ballast bed and the subgrade or formation. The stiffness coefficient of the rail foundation and the rail is also determined by the elastic properties of the rail steel and the actual rail cross-section geometry (from 1.10 m^{-1} to 1.6 m^{-1} is for a track with reinforced concrete sleepers; and from 0.90 m^{-1} to 1.1 m^{-1} is for a track with wooden sleepers).

The stiffness properties of a non-ballasted track have not been thoroughly investigated, which makes it difficult to use the beam model on elastic foundation for the calculation of the track components' SSS. In this regard, it is an urgent engineering task to experimentally determine the stiffness properties of a non-ballasted railway track.

RESEARCH METHODS

Field experiments to determine the modulus of elasticity and correlation stiffness coefficient of rail slab and rails on RHEDA 2000 non-ballasted track were performed on the Sablino – Tosno 46-km section of St. Petersburg – Moscow line (II main track, 45 + 65,00 kilometer post). Non-ballasted track features are shown in *Fig. 2*.

The experiment took place on a track section laid on an embankment of medium-grain sand, with light powdery loam ranging from solid to semi-solid at the base of the embankment. The track consisted of continuous welded P65 rails, VOSSLOH fastenings and German-made sleepers with a layout of 1840 pcs/km. Sleepers were embedded in a load-bearing reinforced B40-class concrete slab of 240 mm thickness. It is laid on a 300-mm-thick foundation slab of B15 concrete. A 40cm-thick protective layer of sand-and-gravel mix is installed under the track foundation slab (*Fig. 2*).

Empty freight trains with the VL10 locomotive, long-distance passenger trains with the EP2K locomotive, ER suburban electric trains, and regional Lastochka ES1high-speed electric trains were running on the section during the experiment. The freight trains' speeds varied between 40–80 km/h, and passenger trains' speeds were between 40–110 km/h.

In order to identify the distance $x = p/4k$ (*Fig. 1*), resistance strain gauges were attached to the bottom edge of the outer rail. The resistance strain gauges conformed to the requirements of GOST 21616 91 "Resistance Strain gauges. General technical requirements". They were attached to the rail bottom with special glue

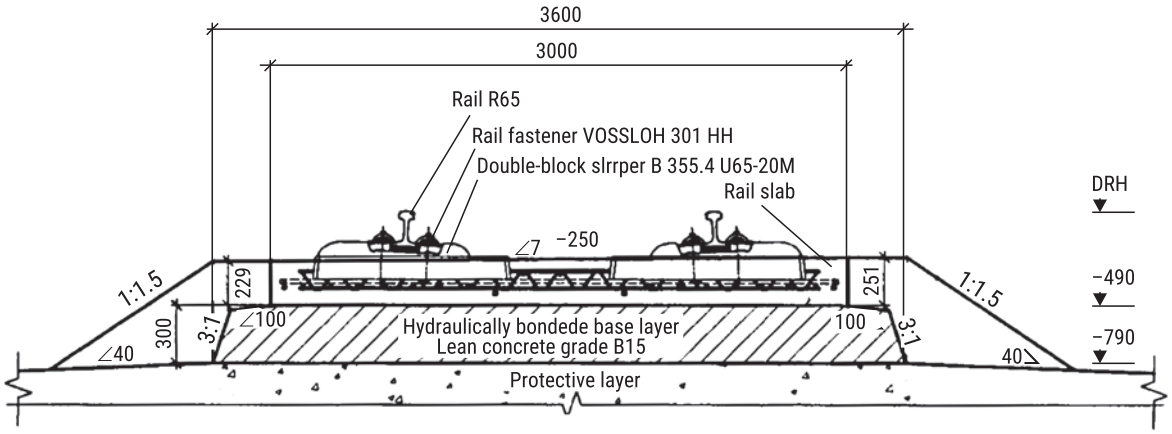

Fig. 2. Design of RHEDA 2000 non-ballasted track system

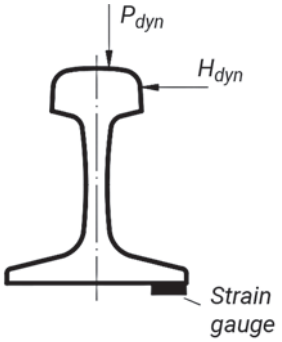

Fig. 3. Strain gauge glued to the rail bottom

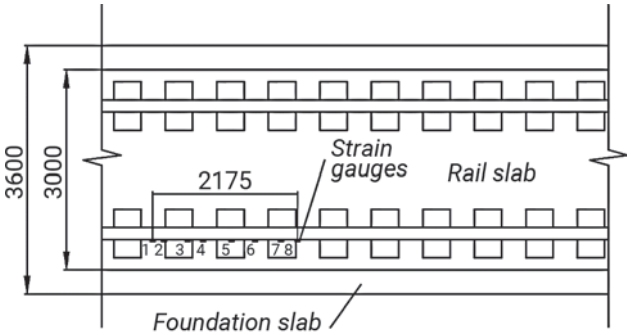

Fig. 4. Lengthwise layout of strain gauges attached to the rail bottom

at a distance of 3 mm from the outer edge of the rail, as shown in *Fig. 3* [9].

The strain gauges were installed every 10–50 cm lengthwise. There were 8 measuring points on a 2.175 m-long rail. The layout of the strain gauges in the experimental section is shown in *Fig. 4*.

The strain gauges were electrically connected in a bridge circuit. An active strain gauge with ohmic resistance R_1 was included in an unbalanced bridge shown in *Fig. 5*.

The measuring circuit was calibrated using a cantilevered beam of equal resistance (*Fig. 6*), onto which strain gauges from the same batch as those used in the experiment were attached with glue [10].

The procedure for calibrating the gauge circuit was as follows: strain gauge R_1 was glued to the bottom edge of the rail, a bridge circuit was assembled, then calibration strain gauge R_2 was connected to one arm, and finally, strain gauges with constant electrical resistance R_3 and R_4 were connected to the other two arms. With the adjustment of R_2 gauge resistance, the bridge circuit was brought to a balanced position, i.e. the value of the current across the diagonal of the bridge was zero. Then a load of certain mass was suspended from the beam with equal resistance thus generating P_i force (*Fig. 6*) and, correspondingly, causing M_i bending moment. The use of a beam with equal resistance showed that the bending stresses $\sigma_{T\text{-}i}$ at any cross-section point are the same when P_i force is applied. Therefore, the bending stresses can be determined by the formula

$$\sigma_{T-i} = \frac{M_i}{W},, \quad (7)$$

where M_i is the bending moment, W is the moment of resistance of the beam with equal resistance.

According to formula (8), the bending moment will be

$$M_i = P_i \cdot l. \quad (8)$$

With the force P_i acting on the beam, the bridge circuit was unbalanced and the current value I_T was detected in the arm of the bridge. Knowing the absolute value of bending stresses in the beam and registering current $I_{T\text{-}i}$, gauge factor $K_{T\text{-}i}$ was determined.

$$K_{T-i} = \frac{\sigma_{T-i}}{I_{T-i}}. \quad (9)$$

Thus, a further research was aimed at determining the bending stresses in the rail σ_p by using a gauge factor to convert the current value in the unbalanced

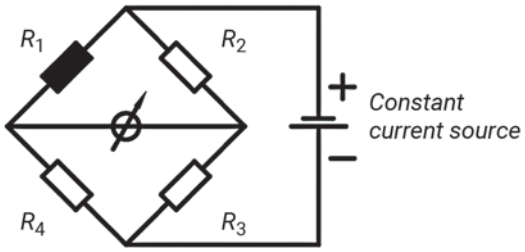

Fig. 5. Bridge connection circuit of strain gauges: R_1 is an active sensor attached to the bottom edge of the rail; R_2 is a calibrating sensor; R_3 and R_4 are resistors with constant electrical resistance

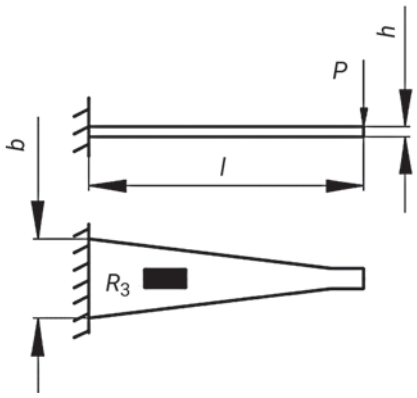

Fig. 6. Cantilever beam of equal resistance for calibrating the measuring circuit: h is beam thickness equal to 0.5 cm; l is beam length equal to 20 cm; b is beam width equal to 8 cm; P is force application point

bridge diagonal Ichan when the wheel-to-rail load was applied

$$\sigma_r = K_T \cdot I_{chan}. \quad (10)$$

During the experiment, the readings of all strain gauges were recorded simultaneously. It allowed processing the results and determining the bending stresses in the rail bottom edges at the same time at different positions of the rolling stock axles relative to the attached strain gauges.

The experimental measurements were processed using conventional methods of mathematical statistics. Statistical series were formed so that one statistical series comprised the values of measured stresses corresponding to one type of rolling stock, fixed axle load and certain train speeds. The probability level in processing the results was assumed 0.994. The main interest was in the mean values of the rail bottom edge stresses, their maximum possible values and the coefficients of variation.

RESEARCH RESULTS

According to the well-known formulae [11], the rail bottom edge stresses can be determined according to the following dependence

$$\sigma_{r-s} = \frac{M_r}{W_r} f, \quad (11)$$

where M_r is the bending moment in the rail caused by the passage of the rolling stock, W_r is the resistance moment in the rail in relation to the furthest fiber at the bottom, f is the transition factor from axial stresses to edge stresses. The value of the latter can be accepted in accordance with the Methodology for assessing the impact of rolling stock on the track to ensure its reliability (RF Railway Ministry, CPT-52/14).

Applying formula (3) in expression (11) including expression (5), we obtain

$$\sigma_{r-s} = \frac{P \cdot f}{4 \cdot k \cdot W_r} \cdot \mu_{kx}. \quad (12)$$

Expression (12) shows that the edge stresses at the rail bottom and the ordinates' influence line of the bending moment will be in direct proportion. Consequently, the edge stresses curve in the rail along its length will coincide with the bending moment curve, while zero edge stresses will be at the point at a distance of $x = \pi/4k$ from the first axis of the train bogie [12]. Recording the movement of the front train bogie axis over the first strain gauge (*Fig. 4*), with the train running from left to right (*Fig. 4*), it is possible to construct the stresses curve in the rail edge acting at the same moment, thereby determining the distance x corresponding to the horizontal coordinate $\pi/4k$ by interpolation (*Fig. 4*). Due to the obtained value of $x = \pi/4k$, the rail slab/rail correlation stiffness coefficient is determined in reverse movement. Modulus of elasticity of the rail slab is calculated using formula (6).

Using this approach and experimental measurements, mean values of the modulus of elasticity of track slab U for different types of rolling stock running at different speeds were calculated. The results are shown in the table below.

DATA ANALYSIS

Based on the data obtained, *Fig. 7* shows the dependencies of the modulus of elasticity of the rail slab on the type of rolling stock and speed changes.

Table

Modulus of elasticity of RHEDA 2000 non-ballasted track

Type of train	Modulus of elasticity of the RHEDA 2000 U non-ballasted track, MPa, at train speeds, km/h						
	от 40 (incl.) до 50 (excl.)	от 50 (incl.) до 60 (excl.)	от 60 (incl.) до 70 (excl.)	от 70 (incl.) до 80 (excl.)	от 80 (incl.) до 90 (excl.)	от 90 (incl.) до 100 (excl.)	от 100 (incl.) до 110 (excl.)
ER electric train	60,0	60,0	59,8	60,0	59,9	59,8	59,5
Lastochka ES electric train	–	–	59,0	58,7	58,9	58,9	58,9
EP2K Locomotive	61,0	60,9	60,8	60,8	60,8	60,7	60,6
VL10 Locomotive	61,0	61,0	61,0	61,0	–	–	–
Passenger car	59,9	59,9	59,8	59,8	59,8	59,8	59,7
Mean	**60,7**	**60,6**	**60,5**	**60,5**	**60,3**	**60,3**	**60,2**
Mean				**60,4**			

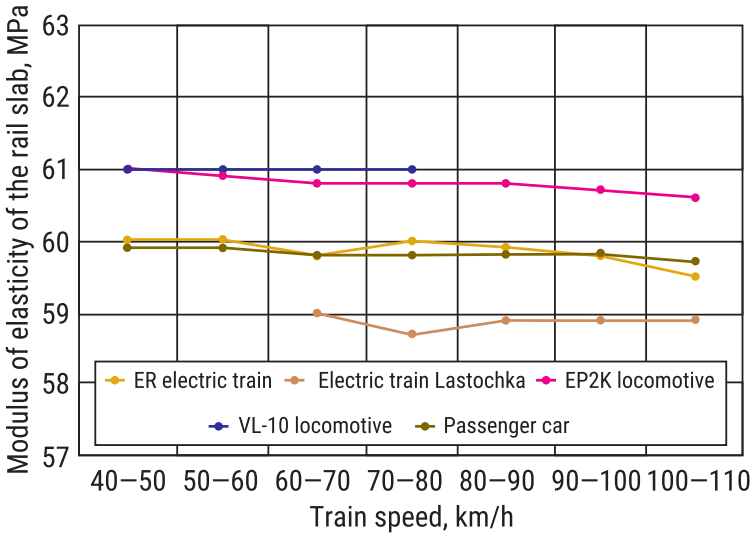

Fig. 7. The effect type of rolling stock and movement speed on the modulus of elasticity of RHEDA 2000 non-ballasted track

The analysis of the experimental data and statistical process results show that the modulus of elasticity of the rail slab varies from 58.9 to 61.0 MPa for all types of rolling stock at different speeds. The discrepancy of the results does not exceed 3–5 % as a rule. For further engineering applications, the modulus of elasticity of RHEDA 2000 non-ballasted track structure can be accepted to be 60 MPa.

A number of scientific papers [13] state that one of the main disadvantages of ballastless track design is considered to be its high stiffness. Track stiffness RT is known to be numerically equal to the force applied to the rail causing its elastic deflection equal to 1, i.e. track stiffness is directly related to the rail slab modulus of elasticity [14].

$$R_{\mathrm{T}} = \frac{2U}{k}. \qquad (13)$$

The experimental results demonstrate that RHEDA 2000 non-ballasted track does not show any significant increase in stiffness compared to a ballasted railway track with reinforced concrete sleepers. The mean value of the modulus of elasticity of the rail foundation for a typical ballasted track is 50–120 MPa [15], whereas for the non-ballasted RHEDA 2000 track it is only 60 MPa. Since the stiffness of the entire track is determined by the stiffness of track elements, the results obtained can be attributed to the use of VOSSLOH W-301-HH fasteners with high elasticity rail pads.

CONCLUSION

The experimental data on determining the modulus of elasticity and rail slab/rail stiffness coefficient of RHEDA 2000 non-ballasted track structure provide a number of key conclusions:

- modulus of elasticity and slab/rail correlation stiffness coefficient for RHEDA 2000 non-ballasted track with train speeds between 40 and 110 km/h do not depend significantly on the type of rolling stock. The variances do not exceed 3–5 %;
- the mean modulus of elasticity of rail slab for RHEDA 2000 non-ballasted track was 60 MPa, which indicates no increase in the stiffness of the ballastless track compared to the ballasted track. The results can be attributed to the use of VOSSLOH W-301-HH fasteners with high elasticity rail pads;
- the obtained elastic properties for RHEDA 2000 rail slab track make it possible to use the model of beam resting on a continuous elastic foundation to determine the strain-stress state of all non-ballasted track components.

REFERENCES

1. Savin A.V., Pevzner V.O., Glyuzberg B.E., Romen Y.S. Roadbed for Ballastless Track. *International Journal of Innovative Technology and Exploring Engineering*. 2019;8(8):593-598.

2. Kazanskaya L., Smirnova O. Influence of Mixture Composition on Fresh Concrete Workability for Ballastless Track Slabs. *E3S Web of Conferences*. 2020;157:06022. DOI: 10.1051/e3sconf/202015706022

3. Dudkin E.P., Zaitsev E.N., Kolankov S.V. Method of Tram Track Structures Feasibility Study. *Procedia Engineering*. 2017;189:854-859. DOI: 10.1016/j.proeng.2017.05.133

4. Kolos A.F., Petrova T.M., Makhonina A.O. Full — Scale Study of Stress-strain State of Ballastless Upper Structure Construction of Rail Way in Terms of Train Dynamic Load. *Procedia Engineering*. 2017;189:429-433. DOI: 10.1016/j.proeng.2017.05.068

5. Volkov A.E., Evard M.E., Volkova N.A., Vukolov E.A. Application of a Microstructural Model to Simulation of a Tini Beam Bending Performance and Calculation of Thickness Stress Distributions. *9th ECCOMAS Thematic Conference on Smart Structures and Materials, SMART 2019*. 2019;686-695.

6. Diachenko L., Benin A., Diachenko A. Research of Interaction of the "Train – Bridge" System with Bridge Deck Resonant Vibrations. *MATEC Web of Conferences*. 2018;239:05002. DOI: 10.1051/matecconf/201823905002

7. Savin A.V., Brzhezovskiy A.M., Tret'yakov V.V., Smelyanskiy I.V., Tolmachev S.V. Investigation of Track Superstructure Ballastless Design. *Russian Railway Science Journal*. 2015;(6):23-32. (In Russ.).

8. Chernyaev E., Cherniaeva V., Blazhko L., Ganchits V. Analysis of Residual Deformations Accumulation Intensity Factors of the Railway Track Located in the Polar Zone. *Lecture Notes in Civil Engineering*. 2020;381-388. DOI: 10.1007/978-981-15-0450-1_39

9. Dudkin E.P., Andreeva L.A., Sultanov N.N. Methods of Noise and Vibration Protection on Urban Rail Transport. *Procedia Engineering*. 2017;189:829-835. DOI: 10.1016/j.proeng.2017.05.129

10. Michas G. Slab Track Systems for High-speed Railways. Division of Highway and Railway Engineering. *Department of Transport Science School of Architecture and the Built Environment. Royal Institute of Technology*. Stockholm, 2012;25-27.

11. Boronenko Yu.P., Rahimov R.V., Lafta W.M., Dmitriev S.V., Belyankin A.V., Sergeev D.A. Continuous Monitoring of the Wheel-rail Contact Vertical Forces by Using a Variable Measurement Scale. *2020 Joint Rail Conference*. 2020. DOI: 10.1115/JRC2020-8067

12. Kolos A., Darienko I., Konon A. Mathematical Model for Forecasting of Rail Track Ballast Bearing Capacity. *Procedia Engineering*. 2017;189:916-923. DOI: 10.1016/j.proeng.2017.05.142

13. Savin A.V., Korolev V.V., Shishkina I.V. Determining Service Life of Non-ballast Track Based on Calculation and Test. *IOP Conference Series: Materials Science and Engineering*. 2019;687(2):022035. DOI: 10.1088/1757-899X/687/2/022035

14. Schilder R., Diederich D. Installation Quality of Slab Track – A Decisive Factor for Maintenance Text. *RTR Special*. Austria, 2007;76-78.

15. Wang P., Xu H., Chen R., Xu J. Effects Analysis of Cracking of CRTS II Slab Track on Subgrade. *Xinan Jiaotong Daxue Xuebao/Journal of Southwest Jiaotong University*. 2012;47(6):929-934. DOI: 10.3969/j.issn.0258-2724.2012.06.004

Bionotes

Ksenia I. Ivanova — Teaching Assistant of the Department "Construction of Roads of Transport Complex"; **Emperor Alexander I St. Petersburg State Transport University (PSTU)**; 9 Moskovsky pr., St. Petersburg, 190031, Russian Federation; kivanova@pgups.ru;

Alexey F. Kolos — Head of the Department "Construction of Roads of the Transport Complex"; **Emperor Alexander I St. Petersburg State Transport University (PSTU)**; 9 Moskovsky pr., St. Petersburg, 190031, Russian Federation; kolos2004@inbox.ru;

Xintong Wang — postgraduate student of the Department "Construction of Roads of Transport Complex"; **Emperor Alexander I St. Petersburg State Transport University (PSTU)**; 9 Moskovsky pr., St. Petersburg, 190031, Russian Federation; wangxintong@mail.ru.

Contribution of the authors: the authors contributed equally to this article.
The authors declare no conflicts of interests.

Corresponding author: Ksenia I. Ivanova, kivanova@pgups.ru.

The article was submitted 14.07.2022; approved after reviewing 18.08.2022; accepted for publication 30.02.2023.